

Resonant valence-to-core x-ray fluorescence spectroscopy on PrO_2

This article has been downloaded from IOPscience. Please scroll down to see the full text article.

1997 J. Phys.: Condens. Matter 9 8155

(<http://iopscience.iop.org/0953-8984/9/38/019>)

View [the table of contents for this issue](#), or go to the [journal homepage](#) for more

Download details:

IP Address: 171.66.16.209

The article was downloaded on 14/05/2010 at 10:36

Please note that [terms and conditions apply](#).

Resonant valence-to-core x-ray fluorescence spectroscopy on PrO₂

S M Butorin^{†§}, L-C Duda^{†||}, J-H Guo[†], N Wassdahl[†], J Nordgren[†],
M Nakazawa[‡] and A Kotani[‡]

[†] Department of Physics, Uppsala University, Box 530, S-751 21 Uppsala, Sweden

[‡] Institute for Solid State Physics, University of Tokyo, Roppongi, Minato-ku, Tokyo 106, Japan

Received 16 May 1997

Abstract. The results of $4f \rightarrow 3d$ x-ray fluorescence measurements, performed with monochromatic-photon excitation at Pr $M_{4,5}$ absorption edges of PrO₂, are presented and discussed in the framework of an Anderson impurity model. The dependence of the fluorescence structures on varying excitation energies is found to be in agreement with the localized, many-body description of the fluorescence process. Experimental spectra are reproduced by model calculations using values for the model parameters in the ground state of the system which are somewhat different from those obtained earlier in an analysis of core-level photoemission and absorption. Referring to this difference, the importance of resonant x-ray fluorescence data for the spectroscopic analysis of strongly correlated systems and for deriving a unique set of model parameters is stressed.

For strongly electron-correlated systems, the fitting of high-energy spectroscopic data is often used to obtain average values of the energy- and configuration-dependent model parameters in the Anderson impurity Hamiltonian (AIH). These parameters are then employed to characterize the ground-state properties of the system. In order to avoid strong renormalization effects for model parameters it is important to use those spectroscopic techniques where the final states of the spectroscopic process are coupled to the ground state itself in the AIH. Resonant valence-to-core x-ray fluorescence spectroscopy (RXFS) of correlated systems has been shown [1–3] to probe low-energy excitations, so the final states reached via creation–annihilation of a core hole can be described by the ground-state AIH. Therefore, the simulation of RXFS data makes it possible to derive values of model parameters for the ground state of the system with higher accuracy [4].

In the present paper we apply RXFS to PrO₂ which is considered to be a strongly covalent compound. Both the localized approach [5, 6], based on the AIH, and band theory [7] were used to describe the electronic structure of this oxide. While some experimental data such as, for example, optical conductivity curves of PrO₂ [8] were found to be in agreement with the results of the local-density-approximation band-structure calculation [7], various core-level photoemission and absorption spectra of this oxide were successfully reproduced using the AIH formalism [5, 6]. In turn, we will show that RXFS data for PrO₂

[§] Also at: MAX-Lab, University of Lund, Box 118, S-221 00 Lund, Sweden. On leave from: Institute of Metal Physics, Ekaterinburg, Russia.

^{||} Present address: Department of Physics, Boston University, Boston, MA 02215, USA.

can be described within the framework of the Anderson impurity model, but the ground-state values of the model parameters derived from our analysis are different from those obtained previously by fitting the core-level spectroscopic data [5, 6]. The main reason for the difference is a significant reduction of the Pr 4f–O 2p hybridization strength in the presence of a core hole [9]. This reduction affects the values of other parameters.

The experiment was carried out at undulator beamline BW3 at HASYLAB, DESY, Hamburg, with a modified SX-700 monochromator [10], utilizing an end station described in reference [11]. A high-resolution, grazing-incidence grating spectrometer [12] with a two-dimensional detector was used to measure the fluorescence.

The PrO₂ sample was prepared as described in reference [13] and was examined with the x-ray diffraction method. Prior to measurements, the finely ground powder of PrO₂ was pressed onto an aluminium substrate and inserted into the analysing chamber through the load-lock system. When taking data the vacuum base pressure was about 5×10^{-9} Torr.

The Pr 4f \rightarrow 3d x-ray fluorescence spectra of this sample were recorded using the second-order diffraction of a 1200 lines mm⁻¹ grating ($R = 5$ m) with a spectrometer resolution of approximately 1.2 eV. The incidence angle of the photon beam was about 15° from the sample surface and the spectrometer was placed horizontally at an angle of 90° with respect to the incidence beam. For energy calibration, the Cu 3d, 4s \rightarrow 2p lines of a pure metal were recorded in second order. To determine the excitation energies, absorption spectra at the Pr 3d edge were measured by means of the total electron yield. The x-ray fluorescence and absorption spectra were brought onto a common energy scale using the elastic peak at the excitation energy set below the Pr 3d edge. During x-ray absorption and fluorescence measurements, the resolution of the monochromator was set to about 0.5 eV and 1.3 eV, respectively.

The Pr 4f \rightarrow 3d x-ray fluorescence spectra of PrO₂ recorded at different excitation energies across the Pr M_{4,5} absorption edges are displayed in figure 1. Spectral structures, which follow increasing excitation energies, can be associated with resonant fluorescence, while those appearing at the constant energy of emitted photons represent normal fluorescence. Resonant fluorescence exhibits strong changes in its spectral shape with varying excitation energies. For 927.7 eV and 930.5 eV exciting photons, the 4f \rightarrow 3d fluorescence spectra take the form of a recombination line with a low-energy shoulder. When the excitation energy increases to 933.3 eV, the shoulder develops into a structure whose relative intensity is higher than that of the recombination line. The latter line becomes weak for the excitation energy set to the M₅ absorption satellite at 937.0 eV. At the same time, the energy separation between the recombination peak and the low-energy prominent structure increases.

A similar trend in the variation of the 4f \rightarrow 3d spectral shape is observed when the excitation energy is tuned across the 3d_{3/2} threshold. Nevertheless, some differences can be seen between the two series of spectra measured with the excitation at the M₅ and M₄ edges, respectively. Thus, for the excitation energy set to the main M₄ absorption peak at 949.7 eV, the low-energy shoulder in the 4f \rightarrow 3d spectrum is more pronounced than the one in the spectrum excited with 930.5 eV photons (the energy of the main M₅ peak). On the other hand, for the excitation energy set to the M₄ absorption satellite at 955.9 eV, the relative intensity of the recombination line is more intense than that for the excitation at the M₅ satellite (937.0 eV).

The observed changes in resonant Pr 4f \rightarrow 3d fluorescence spectra of PrO₂ are similar to those in Ce 4f \rightarrow 3d spectra of CeO₂ [1, 4] recorded at various excitation energies across the Ce 3d_{5/2,3/2} thresholds. For the latter oxide, spectral changes were interpreted within a localized many-body approach based on the AIH. In particular, the appearance of a resonant

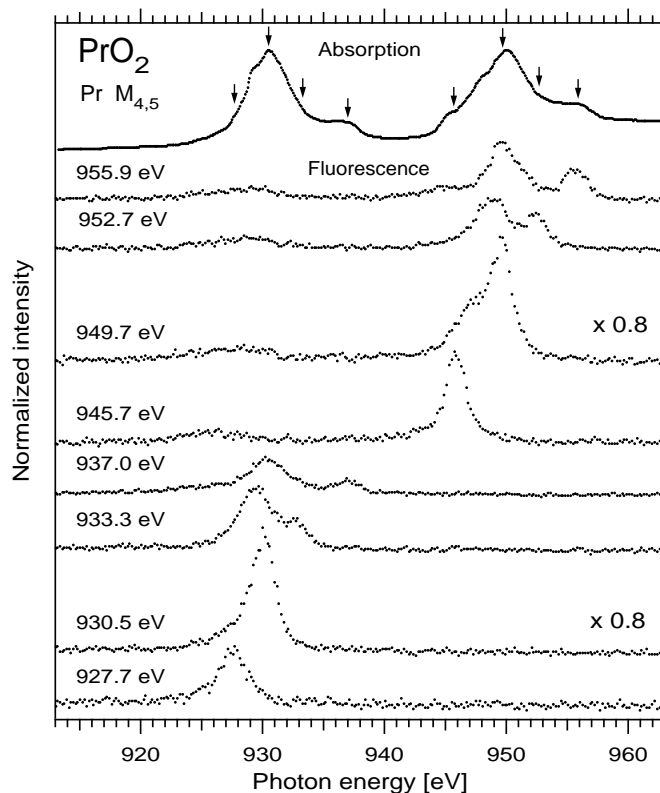


Figure 1. The total-electron-yield spectrum near the Pr 3d edge, and resonant Pr 4f \rightarrow 3d x-ray fluorescence spectra of PrO₂. The fluorescence spectra are normalized to the photon flux. The arrows on the total-electron-yield spectrum indicate the excitation energies used for the fluorescence spectra.

fluorescence structure below the recombination peak for formally tetravalent Ce was shown to be a consequence of the configuration mixing in the ground and core-excited states of the system. The enhancement of this low-energy structure at excitation energies set to satellites in the Ce M_{4,5} absorption edges was attributed to resonances of anti-bonding states between the 4f⁰ and 4f¹ \bar{v} configurations, where \bar{v} represents a hole in the O 2p valence band. The same approach can be applied to the description of the resonant 4f \rightarrow 3d fluorescence process in PrO₂.

Due to strong Pr 4f–O 2p hybridization the initial and intermediate states of this fluorescence process can be described as mixtures of primarily 4f¹ and 4f² \bar{v} and 3d⁹4f² and 3d⁹4f³ \bar{v} configurations, respectively. Then, the main radiative transitions are the ones to the bonding (the recombination line), non-bonding and anti-bonding (the low-energy structures) states [4] between 4f¹ and 4f² \bar{v} configurations, and spectral changes with varying excitation energies are attributed to variations in the rates of transition to these final states.

The important quantity which can be derived from resonant 4f \rightarrow 3d x-ray fluorescence data is the energy separation between the bonding and anti-bonding states for coupled 4f¹ and 4f² \bar{v} configurations in PrO₂. This energy separation is determined by the values of the O 2p \rightarrow Pr 4f charge-transfer energy Δ and the covalency hybridization strength V in the ground state of the system. As for CeO₂, transitions to the anti-bonding states are expected

to be enhanced for the excitation energy set to the Pr $M_{4,5}$ absorption satellites which are in turn the anti-bonding combinations between $3d^94f^2$ and $3d^94f^3\bar{v}$ configurations [5]. Indeed, for 937.0 eV and 955.9 eV exciting photons, the low-energy structure in the Pr $4f \rightarrow 3d$ spectra of PrO_2 is intense and peaks at about 6.5 eV below the recombination line.

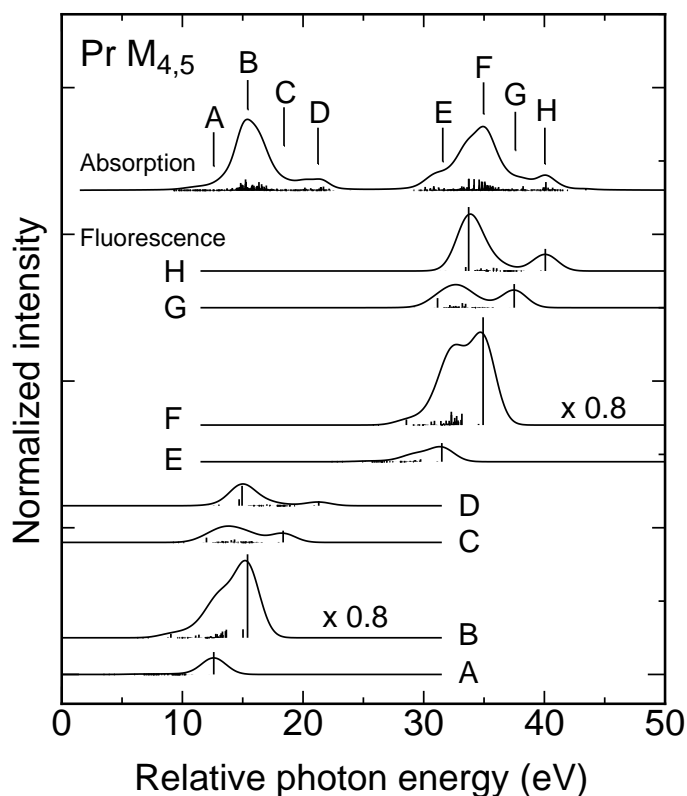


Figure 2. The calculated Pr 3d x-ray absorption and resonant Pr $4f \rightarrow 3d$ x-ray fluorescence spectra of PrO_2 .

The suggested description of the resonant fluorescence process and assignments made for different features in the Pr $4f \rightarrow 3d$ spectra of PrO_2 are supported by the results of calculations within the AIH formalism. These results are shown in figure 2. The calculations were done using a coherent second-order optical formula similar to that used in the analysis of Ce $4f \rightarrow 3d$ spectra of CeO_2 [1, 4]. We included the two configurations $4f^1$ and $4f^2\bar{v}$ for the ground and final states, and $3d^94f^2$ and $3d^94f^3\bar{v}$ for the intermediate state. The values used for the model parameters are as follows: $V = 0.8$, $\Delta = 0.5$, $U_{fc} - U_{ff} = 3.0$ (in units of eV), where Δ is the average value of the energy difference between $4f^2\bar{v}$ and $4f^1$ configurations, U_{fc} is the magnitude of the core-hole potential acting on the $4f$ electron, and U_{ff} is the Coulomb interaction between $4f$ electrons. Furthermore, we simulated the configuration-dependent hybridization using a reduction factor $R_c = 0.7$, so the hybridization between $3d^94f^2$ and $3d^94f^3\bar{v}$ configurations is given as $R_c V$. The effect of multiplet coupling was taken into account in the manner described in reference [5]. The 3d-hole lifetime broadening Γ was assigned the value 0.4 eV. The incident light was assumed to be unpolarized for simplicity. The calculated Pr 3d x-ray absorption and

Pr $4f \rightarrow 3d$ fluorescence spectra were broadened with a Gaussian which has values of the half-width at half-maximum of 0.5 eV and 1.2 eV, respectively.

The calculated results are in overall agreement with experimental data. Some differences in integrated intensities between the experimental and calculated fluorescence spectra which can be seen in figures 1 and 2 are due to self-absorption and saturation [14] effects as well as due to the finite spread of the excitation energy, neglected in the calculations. The calculated final-state multiplet of radiative transitions shows a distinct separation of both bonding and anti-bonding states from a band of continuous states located in between them. The development of the low-energy shoulder in the experimental fluorescence spectra into a prominent structure, separated by ~ 6.5 eV from the recombination line, with increasing excitation energies is seen as a result of variations in the rates of transition to the same set of final states. The calculations also reproduce the differences between the two series of $4f \rightarrow 3d_{5/2}$ and $4f \rightarrow 3d_{3/2}$ spectra which were discussed above.

Using the estimated parameter values, the weights of the $4f^1$ and $4f^2\bar{v}$ configurations in the ground state are calculated to be 0.48 and 0.52, respectively, thus yielding 1.52 electrons for the $4f$ occupancy. This value is in agreement with the one (1.54 electrons) derived from first-principles calculations [15].

It is to be noted that the parameter values (except for that of Δ) in the present calculations are somewhat different from those obtained earlier in the analysis of core-level photoemission and absorption spectra [5]: $V = 0.45$, $\Delta = 0.5$, $U_{fc} - U_{ff} = 2.5$ (in units of eV). The discrepancy is caused by a reduction of V in the presence of a core hole [9] which in turn leads to renormalization effects for other parameters. It is not easy to estimate the value of this reduction on the basis of core-level spectroscopic data alone. Such spectroscopic studies are likely to give values for V in the ground state that are significantly uncertain. On the other hand, RXFS basically probes states as eigenvalues of the ground state AIH, so there are radiative transitions to the ground state itself and low-lying excited states coupled to it. The determination of energies for radiative transitions to the bonding, non-bonding and anti-bonding states between different electronic configurations, contributing to the ground state, puts additional restrictions on the values of V , Δ and U_{ff} . All of this indicates the importance of RXFS for estimating the model parameter values in the ground state of strongly correlated systems, although a unique set of the parameters can be established only by means of a consistent description of the whole variety of spectroscopic and transport properties.

In conclusion, resonant Pr $4f \rightarrow 3d$ x-ray fluorescence measurements and the corresponding theoretical analysis were performed in order to study the effects of Pr $4f$ -O $2p$ hybridization in PrO_2 . The observed agreement between the calculated and experimental spectra supports the validity of the many-body approach based on the Anderson impurity model for the interpretation of resonant Pr $4f \rightarrow 3d$ fluorescence in this oxide. The results obtained clearly demonstrate the efficiency of RXFS in probing the O $2p \rightarrow$ Pr $4f$ charge-transfer excitations and in deriving the values of model parameters in the ground state of the system.

Acknowledgments

The authors would like to thank Dr H Ogasawara for valuable discussions. This work was supported by the Swedish Natural Science Research Council, the Göran Gustavsson Foundation for Research in Natural Sciences and Medicine, and a Grant-in-Aid for Scientific Research from the Ministry of Education, Science, Sports and Culture in Japan.

References

- [1] Butorin S M, Mancini D C, Guo J-H, Wassdahl N, Nordgren J, Nakazawa M, Tanaka S, Uozumi T, Kotani A, Ma Y, Myano K E, Karlin B A and Shuh D K 1996 *Phys. Rev. Lett.* **77** 574
- [2] Butorin S M, Guo J-H, Magnuson M, Kuiper P and Nordgren J 1996 *Phys. Rev. B* **54** 4405
- [3] Butorin S M, Guo J-H, Magnuson M and Nordgren J 1997 *Phys. Rev. B* **55** 4242
- [4] Nakazawa M, Tanaka S, Uozumi T and Kotani A 1996 *J. Phys. Soc. Japan* **65** 2303
- [5] Ogasawara H, Kotani A, Okada K and Thole B T 1991 *Phys. Rev. B* **43** 854
- [6] Bianconi A, Kotani A, Okada K, Giorgi R, Gargano A, Marcelli A and Miyahara T 1988 *Phys. Rev. B* **38** 3433
- [7] Koelling D D, Boring A M and Wood J H 1983 *Solid State Commun.* **47** 227
- [8] Kimura S, Arai F and Ikezawa M 1996 *J. Electron. Spectrosc.* **78** 135
- [9] Gunnarsson O and Jepsen O 1988 *Phys. Rev. B* **38** 3568
- [10] Möller T 1993 *Synchrotron Radiat. News* **6** 16
- [11] Guo J-H, Wassdahl N, Skytt P, Butorin S M, Duda L-C, Englund C J and Nordgren J 1995 *Rev. Sci. Instrum.* **66** 1561
- [12] Nordgren J, Bray G, Cramm S, Nyholm R, Rubensson J-E and Wassdahl N 1989 *Rev. Sci. Instrum.* **60** 1690
- [13] Sawyer J O, Hyde B G and Eyring L 1965 *Bull. Soc. Chim. Fr., Coll. Int.* (Paris: CNRC) p 1190
- [14] Eisebitt S, Böske T, Rubensson J-E and Eberhardt W 1993 *Phys. Rev. B* **47** 14 103
- [15] McMahan A K and Martin R M 1988 *Narrow-Band Phenomena—Influence of Electrons with Both Band and Localized Character* ed J C Fuggle, G A Sawatzky and J W Allen (New York: Plenum) p 133